JOURNAL OF CATALYSIS 14, 4–22 (1969)

Influence of the Surface Structure of a Nickel Oxide Catalyst on the Mechanism of the Room-Temperature Oxidation of Carbon Monoxide

G. EL SHOBAKY,* P. C. GRAVELLE, AND S. J. TEICHNER

From the Institut de Recherches sur la Catalyse (C.N.R.S.), 69 Villeurbanne, France

Received January 16, 1968

The oxidation of carbon monoxide has been studied at 30°C on a nickel oxide prepared by dehydration at 200°C and 10^{-6} torr of a pure nickel hydroxide [NiO(200)], on a nickel oxide prepared at 250°C [NiO(250)], and on nickel oxides with lithium or gallium additions [NiO(Li)(250) and NiO(Ga)(250)]. The slowest step of the overall reaction, in the case of NiO(250) and NiO(Ga)(250), is the interaction between adsorbed oxygen and carbon monoxide, whereas, in the case of NiO(200) and NiO(Li)(250), the slowest step is the interaction between CO_3^-(ads) ions and carbon monoxide. It is concluded that the catalytic activity in the oxidation of carbon monoxide, which follows the sequence NiO(200) < NiO(Li)(250) < NiO(Ga)(250) ⩽ NiO(250), is related rather to the surface defect structure and to the energy distribution of the surface adsorption sites than to the electronic structure of the catalysts.

INTRODUCTION

The catalytic activity of a given catalyst towards a given reaction can be correlated with one of two combined aspects of its surface properties, the chemical aspect or the physical aspect. In the chemical approach, the energy and the nature of the bonds between chemisorbed species involved in the reaction and the catalyst surface are correlated primarily with the chemical nature of these species and with the chemical nature of the surface. On the catalyst surface, which is most often nonhomogeneous, the energy of the bonds for a given adsorbate depends on the adsorption centers: ions or lattice defects of thermal origin or resulting from the previous history of the catalyst. Chemisorption of a reagent on a heterogeneous surface usually reveals the existence of a whole spectrum of sites of various nature and energy (the "energy spectrum" of the surface).

In the physical approach, the catalytic activity of a semiconducting oxide is usually correlated with the position of the Fermi level, which is a collective property. This correlation may be studied for a given reaction on a series of catalysts with different Fermi levels, only if the energy spectrum of their surfaces (their "nonhomogeneity") is well defined and identical. If this condition is not observed, both chemical and physical aspects may interfere in the activity of a given series of catalysts.

With emphasis placed upon the role that the surface structure of any catalyst exerts on its catalytic activity, we investigated, by a microcalorimetric method, the room-temperature oxidation of carbon monoxide on a series of pure and doped nickel oxides of a very high activity, prepared at fairly low temperatures in order to allow a comparison with active industrial catalysts which are never sintered.

The work carried out at Bristol by Garner and his co-workers [for a review, see ref. (*1*)], has already shown how thermochemical data obtained by adsorption calorimetry can be used to deduce the structure of intermediates at a catalyst surface. The sum of the heats released or

* Present address: National Research Center, Dokki, Cairo, U. A. R.

absorbed during the different steps of the actual reaction mechanism is evidently equal to the heat of the noncatalyzed reaction at the same temperature. Experimental heats of adsorption, desorption, and surface interactions must be in agreement, therefore, with the proposed reaction scheme. However, the picture may be somewhat obscured by surface interactions or adsorptions which do not eventually yield the final reaction product, especially if only integral heats of adsorption, desorption, and interaction are measured and compared, as in most of the earlier work. We therefore measured differential heats, which give a picture of the energy spectrum of the surface, and, in the following discussion, agreement between the experimental heats and the thermochemical data is tested for different surface coverages in order to compare the activity of different surface fractions. This method is used here for the first time not only to determine precisely the most probable reaction path but also to determine which part of the surface is actually active during the catalytic process in the formation of the reaction products.

Experimental

Pure nickel oxide was prepared by decomposition of nickel hydroxide *in vacuo* (10^{-6} torr) at 200°C [NiO(200)] or 250°C [NiO(250)] (*2*). Catalysts doped by Li^+ or Ga^{3+} ions were prepared by dehydration of a homogeneous mixture of $Ni(OH)_2$ and lithium or gallium hydroxide at 250°C *in vacuo* [NiO(Li)(250) and NiO(Ga)(250)] (*3*). Different properties of the samples are summarized in Table 1. The composition of all oxides maintained under vacuum is close to the normal stoichiometry. However, NiO(200) and NiO(Li)(250) show a small excess of oxygen whereas NiO(250) and NiO(Ga)(250) contain metallic nickel. Magnetic measurements (*4*) have confirmed the chemical analysis (*5*). All oxides but NiO(Ga)(250) are *p*-type semiconductors (*3*). The electrical conductivity of NiO(Ga)(250) is too small for precise Seebeck-effect measurements.

The following doping mechanisms account for the properties of the doped samples. These mechanisms have been discussed elsewhere (*3*, *6*).

$$(Ni_i^{2+})(O_i^{2-}) + \tfrac{1}{2}nLi_2O \rightarrow (Ni_i^{2+}Li_n^{+})(O_{1+\frac{1}{2}n}^{2-}\square_{a,\frac{1}{2}n})$$

$$(Ni_i^{2+})(O_i^{2-}) + \tfrac{1}{2}nGa_2O_3 \rightarrow (Ni_{i-\frac{1}{2}n}^{2+}Ga_n^{3+}\square_{c,\frac{1}{2}n})(O_{1+n}^{2-}) + \tfrac{1}{2}nNi^0 + \tfrac{1}{4}nO_2(g)$$

Here $\square_a$ and $\square_c$ represent, respectively, an anionic and a cationic vacancy. It should be noted that only a small fraction of the doping agent is incorporated, probably in the surface lattice of nickel oxide (2 at. % Li, in the case of Li^+ ions,

TABLE 1
Properties of Catalysts

Property	NiO(200)	NiO(250)	NiO(Li)(250)	NiO(Ga)(250)
Composition	NiO, 0.155 H_2O	NiO, 0.11 H_2O	NiO, 0.13 H_2O, 0.0475 Li_2O	NiO, 0.14 H_2O, 0.050 Ga_2O_3
Stoichiometry	0.016 at. % O (exc.)	0.033 at. % Ni (exc.)	0.052 at. % O (exc.)	0.049 at. % Ni (exc.)
Electrical conductivity *in vacuo* (ohm^{-1} cm^{-1})				
at 24°C	$\leq 10^{-13}$	$\leq 10^{-13}$	6.2×10^{-12}	$\leq 10^{-13}$
at 200°C	1.6×10^{-10}	2×10^{-10}	6.1×10^{-8}	2.3×10^{-12}
at 250°C	—	1.2×10^{-9}	3.2×10^{-7}	4.5×10^{-11}
Apparent energy of activation of conductivity (kcal/mole)	24 (175–200°C)	24 (175–250°C)	15 (175–250°C)	30 (175–250°C)
Surface area (m^2/g)	142 ± 7	156 ± 7	176 ± 8	151 ± 7

compared with 10 at. % Li in the initial mixture) (*3*).

Measurements of the differential heats of adsorption of reagents were performed in a Calvet microcalorimeter with a precision of 2 kcal/mole (*7*). For each adsorption, small doses of gas were allowed to interact with the sample placed in the calorimeter maintained at 30°C. Electrical conductivities were measured in a cell with platinum electrodes by means of a DC bridge (*8*).

Results

The chemisorption of reagents and product of the reaction was followed calorimetrically. Initial heats of adsorption and amounts of gas adsorbed at 2 torr are listed in Table 2. Differential heats of adsorption as a function of coverage are presented, for oxygen only, in Fig. 1. Two adsorption sequences were also studied by the same method on all samples: Sequence I (CO, O_2, CO) (Table 3) and Sequence II (O_2, CO) (Table 4 and Fig. 2). Before the adsorption of each successive gas, the catalyst was outgassed at 30°C (10^{-6} torr). During these experiments, the introduction of doses of gas was discontinued when the heat of adsorption or interaction decreased to small values (Fig. 2). For all gases, the adsorption or interaction process for the last doses was then very slow (more than 24 hr) and the precision of the measurement was poor. Consequently, the adsorbed amounts listed in Tables 3 and 4 do not refer to a constant gas pressure. They indicate, however, the quantity of each gas which reacts readily with the surface. A modified Sequence II (O_2, CO, O_2) was reinvestigated on NiO(Li)(250) and NiO (Ga)(250) (Fig. 3). Rates of production of heat in the calorimeter are compared in Fig. 4 for several interactions. Catalytic tests were carried out in the calorimeter by introducing doses of the mixture CO + ½ O_2 (Fig. 5) and in a static reactor (catalyst weight, 50 mg; initial pressure of the stoichiometric mixture CO + ½ O_2, 3 torr; liquid nitrogen trap to condense CO_2) (Fig. 6). Electrical conductivity measurements are presented in the following section.

Discussion of the Results

The results of investigations of the room-temperature oxidation of carbon monoxide on NiO(200) have been presented previously (*9*). They will be recalled briefly in this section.

The heats of chemisorption of oxygen on the four samples of nickel oxide and the total amounts of gas adsorbed at 2 torr are different (Fig. 1, Table 2). These results cannot be correlated (i), with the electrical conductivity of the samples, since NiO(200) and NiO(250), which chemisorb oxygen differently, have identical conductivities (Table 1) or (ii), with the total stoichiometry of the solids, since NiO(Li)(250), which has the highest initial oxygen excess content (Table 1), still chemisorbs the highest quantity of oxygen (Fig. 1).

Oxygen ions are most probably adsorbed on the defects (unrecessed nickel ions) of the NiO surface (*10*). Such defects may exist on the surface of the pure oxide prepared at a fairly low temperature (200°C). A higher temperature of preparation of the pure oxide *in vacuo* (250°C), which increases the surface ionic mobility and enhances the recession of cations

TABLE 2
Chemisorption on Nickel Oxide[a]

Catalyst	Oxygen		Carbon monoxide		Carbon dioxide	
	Q	q	Q	q	Q	q
NiO(200)	60	2.03	42 then 29	5.0	46 then 31	9.4
NiO(250)	80	1.9	29	6.6	29	9.7
NiO(Li)(250)	70	2.7	22	5.0	27	13
NiO(Ga)(250)	58	1.7	29	6.6	28	9.3

[a] Q, Initial heat of adsorption (kcal/mole); q, amount adsorbed at 2 torr (cm^3/g).

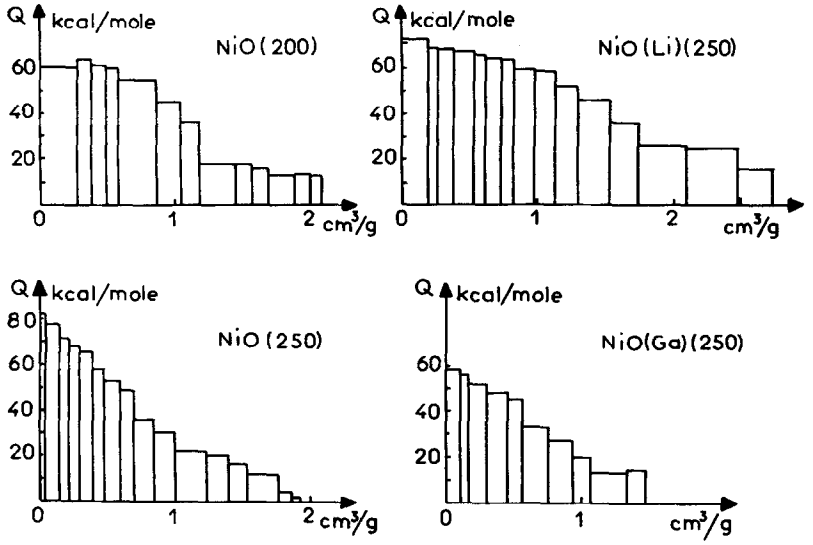

FIG. 1. Adsorption of oxygen on nickel oxides at 30°C.

beneath the oxygen layer, may only decrease the number of such defects. Recession of the cations explains the small decrease of the amount of adsorbed oxygen when the temperature of preparation *in vacuo* of the pure oxide is increased from 200 to 250°C. However, this decrease is not important since, at the temperature of 250°C, anions leave the surface *in vacuo*, forming anionic vacancies, sites for the adsorption of oxygen, and nickel metal (Table 1) (*4*). The metal is not oxidized at 30°C (*4*). Recession of nickel ions and removal of oxygen from different surface regions at 250°C explain the increased heterogeneity which NiO(250) presents during the oxygen adsorption, compared to NiO(200) (Fig. 1). The existence of anionic vacancies on NiO(Li) (250) and of cationic vacancies on NiO(Ga) (250), both types of defects being the result of the incorporation of foreign ions (*3*, *6*), is apparent from the calorimetric results of the chemisorption of oxygen (Fig. 1) since the formation of

TABLE 3
SEQUENCE I OF ADSORPTIONS: CO, O_2, CO

Catalyst	Preadsorbed gas	Adsorbed gas	Initial heat of adsorption (kcal/mole)	Total amount adsorbed with a heat exceeding 6 kcal/mole (cm^3/g)
NiO(200)	—	CO	29	3.00
	CO	O_2	134	2.08
	CO, O_2	CO	65	1.34
NiO(250)	—	CO	29	4.5
	CO	O_2	120	3.78
	CO, O_2	CO	56	2.05
NiO(Li)(250)	—	CO	22	3.5
	CO	O_2	112	4.37
	CO, O_2	CO	64	3.00
NiO(Ga)(250)	—	CO	29	4.5
	CO	O_2	115	3.70
	CO, O_2	CO	52	1.90

TABLE 4
SEQUENCE II OF ADSORPTIONS: O_2, CO

Catalyst	Preadsorbed gas	Adsorbed gas	Initial heat of adsorption (kcal/mole)	Total amount adsorbed with a heat exceeding 6 kcal/mole (cm^3/g)
NiO(200)	—	O_2	60	2.03
	O_2	CO	76	4.98
NiO(250)	—	O_2	80	1.90
	O_2	CO	72	4.70
NiO(Li)(250)	—	O_2	70	2.74
	O_2	CO	68	5.14
NiO(Ga)(250)	—	O_2	58	1.70
	O_2	CO	73	4.50

these surface defects should, as may be observed on Fig. 1, increase the adsorption capacity for oxygen in the case of anionic vacancies and, conversely, decrease it in the case of cationic vacancies. The chemisorption of oxygen may, therefore, be correlated on all samples with the structure of the oxide surface (*6*).

The modification of the surface structure of the NiO catalysts influences less the chemisorption of carbon monoxide or carbon dioxide. A few differences, however, are noted (Table 2). Chemisorption of the first doses of carbon monoxide or carbon dioxide releases on NiO(200) a high heat which is not obtained on nickel oxides prepared at 250°C. This heat results from the interaction of these gases with oxygen ions on NiO(200) which are removed from the surface in vacuum at 250°C (*11*). Incorporation of lithium ions enhances the chemisorption of carbon dioxide and decreases the adsorption capacity for carbon monoxide. Discussion of these results, which shows that they are again related to the structure of the nickel oxide surface, is presented separately (*12*).

The calorimetric measurements give clear evidence of the different surface interactions (Tables 3 and 4) since the heats of adsorption of a gas chemisorbed on a surface precovered by other reagents are very different from those obtained on the pure surface (Table 2). As noted earlier in the text, the amounts of adsorbed gas listed in Tables 3 and 4 do not refer to a constant gas pressure but they indicate the quantity of each gas which reacts readily with the surface with the production of heats exceeding 6 to 8 kcal/mole. Mechanisms of interaction may be determined from the calorimetric data through the use of thermochemical cycles (*13*).

During the adsorption of oxygen on the CO-precovered surfaces (Sequence I), the electrical conductivity of all samples increases [e.g., from 6.2×10^{-12} to 2.4×10^{-7} ohm^{-1} cm^{-1} in the case of NiO(Li)(250)]. During the second adsorption of carbon monoxide, the conductivity decreases [to 9×10^{-9} ohm^{-1} cm^{-1}, in the case of NiO(Li)(250)]. This evolution has been related, in the case of NiO(200) (*9*, *13*), to the intermediate formation of CO_3^-(ads) ions and to their subsequent partial conversion by carbon monoxide to form carbon dioxide which was actually detected in the cold trap. It must also be recalled that CO_3^-(ads) ions formed on the most active sites of the NiO(200) surface, with the production of 134 kcal/mole (Table 3), do not react with carbon monoxide to form either adsorbed or gaseous carbon dioxide (*9*, *13*). These ions inhibit the most active surface sites. The similarity of the heats recorded during the adsorption of oxygen on the four CO-precovered oxides (Table 3) suggests that, in all cases, CO_3^-(ads) ions are formed. Moreover, since the electrical conductivity of none of the samples decreases to its initial value during the second adsorption of carbon monoxide, some

ions, which can only be CO_3^-(ads) ions, still remain on the surface of all oxides at the end of Sequence I. It must be noted also, from Table 3, that the quantity of carbon monoxide (second adsorption), adsorbed on the solids treated previously by carbon monoxide and oxygen, and containing therefore CO_3^-(ads) ions, is not large enough to react with all complex ions formed on their surface. It appears that on all oxides a fraction of CO_3^-(ads) ions does not react with carbon monoxide to yield carbon dioxide and remains undecomposed. It is reasonable to assume that in all cases, as was demonstrated in the case of NiO (200) (*13*), nonreactive CO_3^-(ads) ions are located on the most reactive surface sites and are consequently formed with the production of high heats [134 to 115 kcal/mole in the case of NiO(200)].

The total quantity of CO_3^-(ads) ions is determined by the amount of oxygen which reacts with the CO-precovered surface with the production of heats exceeding the heat of adsorption of oxygen on the fresh oxides. For instance, although 3.78 cm^3 O_2/g is adsorbed readily on the surface of NiO (250) containing preadsorbed carbon monoxide (Table 3), only a fraction (3 cm^3 O_2/g) of this total amount is adsorbed with the production of heats exceeding 80 kcal/mole (Table 2). This fraction only is considered as transformed into CO_3^-(ads) ions. It must be noted that the quantity of preadsorbed carbon monoxide (4.5 cm^3 CO/g, Table 3) exceeds the amount required by the stoichiometry of Eq. [2] to react with this fraction of adsorbed oxygen (3 cm^3 O_2/g) to yield CO_3^-(ads) ions. Similarly, carbon monoxide is assumed to react with CO_3^-(ads) ions (second adsorption of CO), when its adsorption produces heats exceeding that of the adsorption of carbon monoxide on the fresh surface [29 kcal/mole in the case of NiO(250), Table 2]. A quantity of 2 cm^3 CO/g is thus reacting in the case of NiO(250). Since in this case 3 cm^3 O_2/g is transformed into CO_3^-(ads) ions and since 2 cm^3 CO/g only reacts subsequently with these complex ions to form carbon dioxide, it is concluded from the stoichiometry of Eq. [3] (Table 5) that a fraction of CO_3^-(ads) ions corresponding to 1 cm^3 O_2/g remains on the surface of NiO(250). This determination is only approximate but its inaccuracy does not detract from the validity of the following discussion.

Thermochemical cycles may be used to confirm the formation and to verify the subsequent decomposition of reactive CO_3^-(ads) ions (Tables 5 and 6). All heats in the cycles are expressed in kcal/mole and the numbers in parentheses indicate the corresponding surface coverages expressed in cm^3/g. The cycles are tested first (column *a*) at the lowest surface coverage for which conversion of CO_3^-(ads) ions by carbon monoxide to form carbon dioxide becomes probable (1 cm^3 O_2/g, Eq. [2], Tables 5 and 6, in the case of NiO(250) for instance). It is assumed, in each case, that the first doses of a gas interact with preadsorbed reactive species located on the most energetic sites. For instance, it is assumed that when oxygen contacts the CO-precovered samples (Eq. [2]), it reacts first with carbon monoxide species adsorbed (Eq. [1]) on the most reactive surface sites. Adsorption of oxygen on samples containing limited amounts of preadsorbed carbon monoxide have shown indeed that this assumption is correct. The cycles (Tables 5 and 6) are tested also for a higher coverage of the surface by adsorbed species (column *b*). In the case of NiO(250), for instance, the heat of adsorption of carbon monoxide which is then used in the calculation (Eq. [1]) was measured when the surface coverage by this gas was 2.25 cm^3/g. The corresponding heat for oxygen adsorption (108 kcal/mole) was determined for a surface coverage by this gas (2.25 cm^3/g) in agreement with the stoichiometry of the proposed interaction (Eq. [2]). The heat for the second adsorption of carbon monoxide on NiO(250) (30 kcal/mole, Tables 5 and 6) was evaluated for a surface coverage by this gas (1.25 cm^3 CO/g) in agreement with the quantity of *reactive* CO_3^-(ads) ions adsorbed on the catalyst after the interaction of oxygen (2.25 cm^3 O_2/g) with preadsorbed carbon monoxide (2.25 cm^3

TABLE 5

THERMOCHEMICAL CYCLE 1[a]

[1]	$CO(g) \rightarrow CO(ads)$
[2]	$CO(ads) + O_2(g) + Ni^{2+} \rightarrow CO_3^-(ads) + Ni^{3+}$
[3]	$CO_3^-(ads) + CO(g) + Ni^{3+} \rightarrow 2\ CO_2(g) + Ni^{2+}$
$\frac{1}{2}([1] + [2] + [3])$	$CO(g) + \frac{1}{2}\ O_2(g) \rightarrow CO_2(g)$

Interaction	NiO(200)		NiO(250)		NiO(Li)(250)		NiO(Ga)(250)	
	a	*b*	*a*	*b*	*a*	*b*	*a*	*b*
[1]	+20(1)	+8(1.8)	+20(1)	+10(2.25)	+20(0.5)	+7(1.75)	+21(1)	+10(2.25)
2]	+115(1)	+100(1.8)	+118(1)	+108(2.25)	+107(0.5)	+103(1.75)	+115(1)	+110(2.25)
3]	+65(0)	+40(0.8)	+56(0)	+30(1.25)	+64(0)	+35(1.25)	+52(0)	+27(1.25)
$\frac{1}{2}([1] + [2] + [3])$	+100	+74	+97	+74	+95.5	+72.5	+94	+73.5

[a] Figures which are not in parentheses refer to the heats of adsorption or interaction in kcal/mole; figures in parentheses refer to the corresponding surface coverage in cm^2/g. For headings *a* and *b*, see the text.

TABLE 6

THERMOCHEMICAL CYCLE 2[a]

[1]	$CO(g) \rightarrow CO(ads)$
[2]	$CO(ads) + O_2(g) + Ni^{2+} \rightarrow CO_3^-(ads) + Ni^{3+}$
[3]	$CO_3^-(ads) + CO(g) + Ni^{3+} \rightarrow 2\ CO_2(ads) + Ni^{2+}$
[4]	$2\ CO_2(ads) \rightarrow 2\ CO_2(g)$
$\frac{1}{2}([1] + [2] + [3] + [4])$	$CO(g) + \frac{1}{2}\ O_2(g) \rightarrow CO_2(g)$

Interaction	NiO(200)		NiO(250)		NiO(Li)(250)		NiO(Ga)(250)	
	a	*b*	*a*	*b*	*a*	*b*	*a*	*b*
[1]	+20(1)	+8(1.8)	+20(1)	+10(2.25)	+20(0.5)	+7(1.75)	+21(1)	+10(2.25)
[2]	+115(1)	+100(1.8)	+118(1)	+108(2.25)	+107(0.5)	+103(1.75)	+115(1)	+110(2.25)
[3]	+65(0)	+40(0.8)	+56(0)	+30(1.25)	+64(0)	+35(1.25)	+52(0)	+27(1.25)
[4]	−62(0)	−56(1.6)	−58(0)	−52(2.5)	−54(0)	−46(2.5)	−56(0)	−44(2.5)
$\frac{1}{2}([1] + [2] + [3] + [4])$	+69	+46	+68	+48	+68.5	+49.5	+66	+51.5

[a] Figures which are not in parentheses refer to the heats of adsorption or interaction in kcal/mole; figures in parentheses refer to the corresponding surface coverage in cm^3/g. For headings *a* and *b*, see the text.

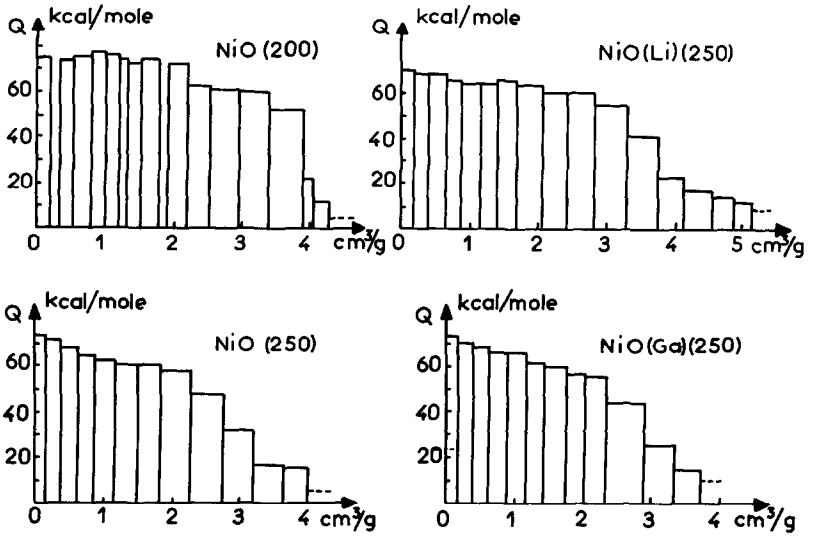

FIG. 2. Adsorption of carbon monoxide at 30°C on nickel oxides precovered by oxygen.

CO/g) and also in agreement with the stoichiometry of Eq. [3]. The interaction of this amount of carbon monoxide (1.25 cm^3 CO/g) with CO_3^-(ads) ions produces 2.50 cm^3 of carbon dioxide per gram of NiO (250) (Eq. [3]). Accordingly, the heat of desorption of carbon dioxide which appears in Cycle 2 (Table 6) is equal, in absolute value, to the heat of adsorption of carbon dioxide on NiO(250) for the same surface coverage (2.50 cm^3 CO_2/g). It has been shown already (*13*) that the heat of adsorption of carbon dioxide is not much modified by the presence of preadsorbed ions. The heat of the homogeneous process being 68 kcal/mole (*14*), Cycle 1 (Table 5) is not balanced for low coverages of the surface of NiO(250) (*a*) but it is balanced for higher coverages (*b*). The same method is applied to test all thermochemical cycles presented in this article.

Cycle 1 (Table 5) tests the formation of gaseous carbon dioxide at the end of Sequence I (see Table 3) and Cycle 2 (Table 6) the formation of adsorbed carbon dioxide for the same sequence. On all samples, CO_3^-(ads) ions are formed through interaction [2] and their subsequent conversion by carbon monoxide yields carbon dioxide. On active sites, carbon dioxide remains adsorbed (Cycle 2, column *a* is balanced in all cases) and acts as an inhibitor for further adsorptions and interactions. On less active sites, carbon dioxide is desorbed to the gas phase (Cycle 1, column *b*) and, in all cases, it is detected in the cold trap. Therefore interactions [1], [2], and [3] of Sequence I (Tables 5 and 6) are the intermediate steps of a possible reaction mechanism (Mechanism I) on all catalysts. On all catalysts also, the most active sites are inhibited either by nonreactive CO_3^-(ads) ions or by adsorbed carbon dioxide.

The chemisorption of oxygen on the fresh surface (Sequence II, Table 4) increases the electrical conductivity of all samples [e.g., from 6.2×10^{-12} to 1.8×10^{-6} ohm^{-1} cm^{-1} in the case of NiO(Li)(250)]. The subsequent adsorption of carbon monoxide (Table 4, Fig. 2) yields neutral species since it decreases the electrical conductivity of all samples to its low initial value (Table 1). The neutral species is carbon dioxide since, for all oxides prepared at 250°C, carbon dioxide is indeed condensed in the cold trap. In the case of NiO (200), it was shown previously that CO_2 (ads) is the *only* species formed under these conditions (*9, 13*). During Sequence II, formation of carbon dioxide may be achieved either through the intermediate formation of CO_3^-(ads) ions

$$2\,O^-(ads) + CO(g) + 2\,Ni^{3+} \rightarrow CO_3^-(ads) + Ni^{2+} + Ni^{3+} \quad [6]$$

followed by interaction [3], or, directly,

$$O^-(ads) + CO(g) + Ni^{3+} \rightarrow CO_2 + Ni^{2+} \quad [7]$$

It must be noted that interaction [7] is equivalent to half the sum of interactions [6] and [3]. Interaction [7] does not, therefore, completely preclude the intermediate formation of CO_3^-(ads) ions but it means only that these complex ions, if they are formed, are not detected by the microcalorimetric technique that we used. Conversely, interaction [6] may be verified from the calorimetric data when the reactivity of the intermediate CO_3^-(ads) ions towards carbon monoxide (Eq. [3]) is low, i.e., when they are not immediately converted by carbon monoxide into gaseous or adsorbed carbon dioxide. Moreover, even in the latter case, the existence of CO_3^-(ads) ions may be ascertained only if the amount of carbon monoxide contacting the oxygen-precovered sample is small compared with the quantity of preadsorbed oxygen, since any excess of carbon monoxide may react with the complex ions, converting them into carbon dioxide.

Thermochemical cycles were used to test separately both hypotheses (Eqs. [6] and [7]). The possibility of the direct formation of adsorbed or gaseous carbon dioxide, through interaction [7], is verified in Cycle 3 (Table 7) and Cycle 4 (Table 8). On NiO(200) and NiO(Li)(250), all carbon dioxide molecules formed according to this interaction remain adsorbed, Cycle 3 (Table 7) being balanced for a low (*a*) or high (*b*) surface coverage. Gaseous carbon dioxide, however, may be formed on NiO (250) and NiO(Ga)(250) when the coverage of their surface by reacting species is high (column *b*, Cycle 4, Table 8). These conclusions are derived from the comparison of the heat of the homogeneous combustion of carbon monoxide (68 kcal/mole) with the heats calculated for the same process in Cycle 3 (adsorbed CO_2, Table 7) and Cycle 4 (gaseous CO_2, Table 8).

Inhibition of the catalytic oxidation of carbon monoxide at room temperature by adsorbed carbon dioxide is thus confirmed since interaction [7] yields adsorbed carbon dioxide on the most reactive sites of all catalysts, and even on the low activity sites of NiO(200) and NiO(Li)(250). Interaction [7] yields, however, gaseous carbon dioxide on the low-energy sites of the NiO(250) and NiO(Ga)(250) surfaces. This interaction may therefore be considered also as an intermediate step of the catalytic reaction on these catalysts. Thus, in addition to Mechanism I, there appears the possibility of a second reaction mechanism (Mechanism II) in which formation of CO_3^-(ads) ions, through interaction [2], is no longer a necessary intermediate step.

The complex ions may also be formed through interaction [6], which is tested in Cycle 5 (Table 9) by assuming that if they are formed these complex ions must be identical to CO_3^-(ads) ions created during interaction [2] in Sequence I. The data of Table 9 show that the formation of the CO_3^-(ads) complex through interaction [6] is indeed possible for a low coverage of NiO(250) and for low and high coverages of NiO(Li)(250). Formation of CO_3^-(ads) ions is precluded for any surface coverage of the two other catalysts. These conclusions are deduced from the comparison of the experimental heats of the adsorption of carbon monoxide and those calculated from Cycle 5 (sum of interactions [5], [6], and [2]).

Let us consider first the case of NiO (250). It may be observed that the formation of CO_3^-(ads) ions through interaction [6] is possible only on a small number of high-energy sites (low coverage, *a*, Table 9; heat of the oxygen adsorption, 80 kcal/mole; Fig. 1), which are probably anionic vacancies (*3*). Formation of CO_3^-(ads) ions on these sites of the NiO(250) surface, through interaction [2], has already been demonstrated. The possibility of the formation of the complex ions through interaction [6] therefore does not change the previous conclusions concerning the occurrence of Mechanism I on this catalyst. But for a high coverage (low-energy sites) of the same catalyst, the direct formation

TABLE 7

THERMOCHEMICAL CYCLE 3[a]

[5]	$\frac{1}{2}\,O_2(g) + Ni^{2+} \rightarrow O^-(ads) + Ni^{3+}$
[7]	$O^-(ads) + CO(g) + Ni^{3+} \rightarrow CO_2(ads) + Ni^{2+}$
[4]	$CO_2(ads) \rightarrow CO_2(g)$
([5] + [7] + [4])	$CO(g) + \frac{1}{2}\,O_2(g) \rightarrow CO_2(g)$

	NiO(200)		NiO(250)		NiO(Li)(250)		NiO(Ga)(250)	
Interaction	*a*	*b*	*a*	*b*	*a*	*b*	*a*	*b*
[5]	+30(0)	+23(1)	+29(0.4)	+11.5(1)	+35(0)	+24(1.4)	+29(0)	+12(0.9)
[7]	+76(0)	+72(2)	+66(0.4)	+58 (2)	+68(0)	+62(2.8)	+73(0)	+60(1.8)
[4]	−31(0)	−27(2)	−27(0.4)	−26 (2)	−27(0)	−23(2.8)	−28(0)	−24(1.8)
([5] + [7] + [4])	+75	+68	+68	+43.5	+76	+63	+74	+48

[a] Figures which are not in parentheses refer to the heats of adsorption or interaction in kcal/mole; figures in parentheses refer to the corresponding surface coverage in cm^3/g. For headings *a* and *b*, see the text.

TABLE 8

THERMOCHEMICAL CYCLE 4[a]

[5]	$\frac{1}{2}\,O_2(g) + Ni^{2+} \rightarrow O^-(ads) + Ni^{3+}$
[7]	$O^-(ads) + CO(g) + Ni^{3+} \rightarrow CO_2(g) + Ni^{2+}$
([5] + [7])	$CO(g) + \frac{1}{2}\,O_2(g) \rightarrow CO_2(g)$

Interaction	NiO(200)		NiO(250)		NiO(Li)(250)		NiO(Ga)(250)	
	a	*b*	*a*	*b*	*a*	*b*	*a*	*b*
5]	+30(0)	+23(1)	+29(0.4)	+11.5(1)	+35(0)	+24(1.4)	+29(0)	+12(0.9)
[7]	+76(0)	+72(2)	+66(0.4)	+58(2)	+68(0)	+62(2.8)	+73(0)	+60(1.8)
([5] + [7])	+106	+95	+95	+69.5	+103	+86	+102	+72

[a] Figures which are not in parentheses refer to the heats of adsorption or interaction in kcal/mole; figures in parentheses refer to the corresponding surface coverage in cm^3/g. For headings *a* and *b*, see the text.

TABLE 9

THERMOCHEMICAL CYCLE 5[a]

[5] $O_2(g) + 2\,Ni^{2+} \rightarrow 2\,O^-(ads) + 2\,Ni^{3+}$

[6] $2\,O^-(ads) + 2\,Ni^{3+} + CO(g) \rightarrow CO_3^-(ads) + Ni^{3+} + Ni^{2+}$

[2] $CO_3^-(ads) + Ni^{3+} \rightarrow CO(ads) + O_2/g) + Ni^{2+}$

([5] + [6] + [2]) = [1] $CO(g) \rightarrow CO(ads)$

Interaction	NiO(200)		NiO(250)		NiO(Li)(250)		NiO(Ga)(250)	
	a	*b*	*a*	*b*	*a*	*b*	*a*	*b*
[5]	+60(0)	+46(1)	+80(0)	+23(1)	+70(0)	+48(1.4)	+58(0)	+24(0.9)
[6]	+76(0)	+76(1)	+72(0)	+63(1)	+68(0)	+67(1.4)	+73(0)	+65(0.9)
[2]	−134(0)	−115(1)	−120(0)	−110(1)	−112(0)	−107(1.4)	−115(0)	−113(0.9)
([5] + [6] + [2])	+2(0)	+7(1)	+32(0)	−24(1)	+26(0)	+8(1.4)	+16(0)	−24(0.9)
[1][b]	+29(0)	+20(1)	+29(0)	+20(1)	+27(0)	+10(1.4)	+28(0)	+20(0.9)

[a] Figures which are not in parentheses refer to the heats of adsorption or interaction in kcal/mole; figures in parentheses refer to the corresponding surface coverage in cm^3/g. For headings *a* and *b*, see the text.

[b] Experimental values.

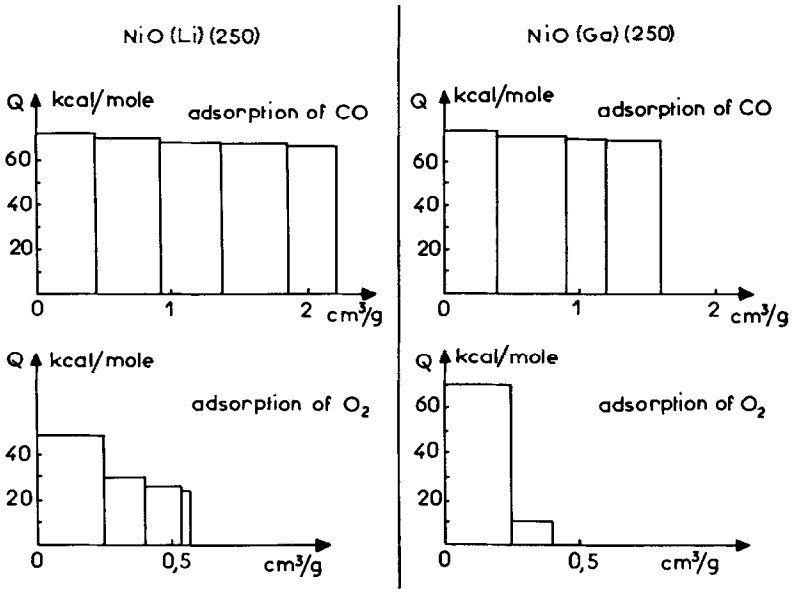

FIG. 3. Successive adsorptions at 30°C of carbon monoxide and then of oxygen on nickel oxides precovered by oxygen.

of gaseous carbon dioxide (interaction [7]) becomes probable and the possibility of another reaction path appears, as seen previously (Mechanism II).

In the case of NiO(Li) (250), interaction [7] should result in the formation of adsorbed carbon dioxide exclusively. This conclusion deduced from Cycle 3 (Table 7) is in disagreement with the experimental evidence since gaseous carbon dioxide is found in the cold trap after the interaction of carbon monoxide with the oxygen-precovered surface (Sequence II). Cycle 5 (Table 9), however, is also balanced. The possibility of the formation of CO_3^-(ads) ions through interaction [6] and of their subsequent conversion into carbon dioxide by excess carbon monoxide must be therefore envisaged. The corresponding reaction mechanism is similar to Mechanism I. Because of the uncertainty of the thermochemical cycles in this case, a careful examination of the conditions of formation of CO_3^-(ads) ions is required.

The formation of relatively stable CO_3^-(ads) ions through interaction [6] should release adsorption sites, whereas the direct formation of adsorbed carbon dioxide through interaction [7] clearly does not release adsorption sites. The presence or absence of free adsorption sites on the NiO (Li) (250) surface during the interaction of carbon monoxide with preadsorbed oxygen was verified by the following experiments. Oxygen (2.6 cm³ O_2/g) was first adsorbed on a sample of NiO(Li) (250) as at the beginning of Sequence II. A limited amount of carbon monoxide (2.2 cm³ CO/g) was then allowed to react with the oxygen-precovered surface (Fig. 3). Oxygen was then adsorbed again on the sample. The initial heat of the second adsorption of oxygen (48 kcal/mole) (Fig. 3) is in good agreement with the heat which is measured during the adsorption of oxygen on the freshly prepared sample (Fig. 1) for the same surface coverage by ionic species [1.5 cm³ O_2/g, since 0.4 cm³ O_2/g remains unaltered and since the coverage by CO_3^-(ads) produced by the reaction of 2.2 cm³ CO/g is considered equivalent to 1.1 cm³ O_2/g]. It is concluded from these experiments that at the beginning of the interaction of carbon monoxide with oxygen preadsorbed on NiO (Li) (250), free sites are released on the surface and that, consequently, this inter-

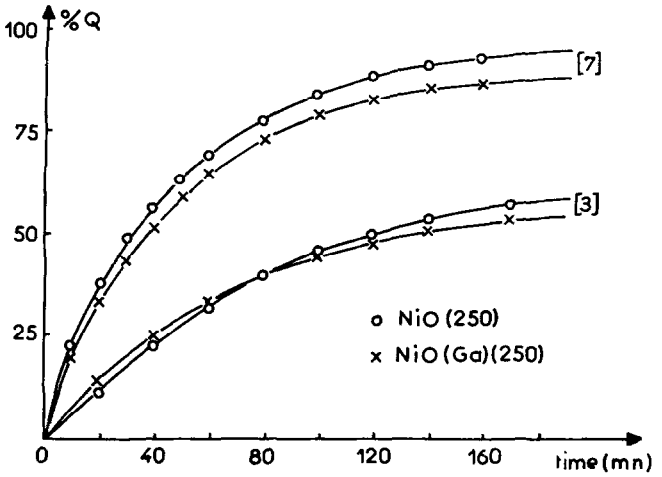

FIG. 4. Rates of production of heat in the calorimeter for interaction [3] (see tables) and for interaction [7] (see Table 7) on the surface of NiO(250) and NiO(Ga)(250).

action produces relatively stable CO_3^-(ads) ions (interaction [6]).

The same experiments were repeated, for comparative purposes, on a sample of NiO (Ga) (250), since it has been shown previously that interaction [6] is precluded on this catalyst. In this case, the initial heat of the second adsorption of oxygen on the sample previously treated by oxygen and then by a limited quantity of carbon monoxide (1.6 cm^3 CO/g) is 70 kcal/mole (Fig. 3). This value, which exceeds even the initial heat of adsorption of oxygen on the freshly prepared sample (Fig. 1), cannot be explained by the adsorption of oxygen on free sites. It is close, however, to the heat released by the interaction of oxygen with a CO_2-precovered nickel oxide (83 kcal/mole) (*13*). This result may be considered as a further proof of the direct formation of carbon dioxide (interaction [7]) on the surface of NiO(Ga) (250) during Sequence II.

Finally, it appears from these results that only one reaction mechanism is probable on NiO(200) (Mechanism I):

$$CO(g) \rightarrow CO(ads) \quad [1]$$
$$CO(ads) + O_2(g) + Ni^{2+} \rightarrow CO_3^-(ads) + Ni^{3+} \quad [2]$$
$$CO_3^-(ads) + CO(g) + Ni^{3+} \rightarrow 2\,CO_2(g) + Ni^{2+} \quad [3]$$

The same mechanism is also probable on the surface of NiO(Li) (250) but, in addition to reaction [2], the complex CO_3^- (ads) ions may be formed through interaction [6]:

$$2\,O^-(ads) + CO(g) + 2\,Ni^{3+} \rightarrow CO_3^-(ads) + Ni^{3+} + Ni^{2+} \quad [6]$$

Calorimetric curves (heat evolved versus time) of the type of Fig. 4 indicate that, on NiO(200) and NiO(Li) (250), conversion of CO_3^-(ads) ions by carbon monoxide (Eq. [3]) is a much slower process than interaction [2]. A kinetic study of the reaction on both catalysts has demonstrated moreover that the reaction rate does not depend on p_{CO} (*9*, *16*). Interaction [3] may therefore be considered as the slowest step of the catalytic reaction in the case of NiO (Li) (250), as was already demonstrated in the case of NiO(200) (*9*).

On NiO(250) and NiO(Ga) (250), two reaction paths are possible simultaneously: Mechanism I, as previously in the case of NiO(200) and NiO(Li) (250), and also the direct formation of gaseous carbon dioxide (Eq. [7]) (Mechanism II):

$$\tfrac{1}{2}\,O_2(g) + Ni^{2+} \rightarrow O^-(ads) + Ni^{3+} \quad [5]$$
$$O^-(ads) + CO(g) + Ni^{3+} \rightarrow CO_2(g) + Ni^{2+} \quad [7]$$

In order to determine which mechanism actually governs the catalytic reaction on NiO(250) and NiO(Ga) (250), it is necessary to compare the rates of the slowest steps of both mechanisms.

As in the case of NiO(200) (*9*) and NiO(Li) (250), calorimetric experiments

show that on the surface of NiO(250) and NiO(Ga) (250) formation of CO_3^-(ads) ions (Eq. [2]) and adsorption of oxygen (Eq. [5]) are fast processes. Interactions [1], [3], and [7] are slower processes. Therefore the slowest step of Mechanism II may be only interaction [7].

Moreover, kinetic results (*16*) have shown that on NiO(250) and NiO(Ga) (250), as previously in the case of NiO(200) (*9*), the reaction rate does not depend on p_{CO}. Adsorption of carbon monoxide on NiO (250) and NiO(Ga) (250) is not the slowest step of the reaction on these catalysts. Thus, the slowest step of Mechanism I, if this mechanism, instead of Mechanism II, governs the catalytic reaction on NiO(250) and NiO(Ga) (250), could only be interaction [3]. The same limiting step was proposed previously for the reaction on NiO (200) (*9*) and on NiO(Li) (250). The rates of production of heat during interactions [3] and [7], which are the slowest steps, respectively, of Mechanisms I and II, are compared in Fig. 4 for NiO(250) and NiO (Ga) (250). This figure shows that interaction [7] is faster. It therefore governs the catalytic reaction and, on both catalysts, Mechanism II prevails.

The catalytic reaction itself was also studied calorimetrically by introducing successive doses of the stoichiometric reaction mixture to the catalyst in the calorimeter (*13*). Rates of production of heat for several doses are plotted in Fig. 5. On all catalysts, the rate decreases when an increasing amount of mixture has reacted (curves A to C, Fig. 5). This confirms that carbon dioxide inhibits the catalysts (*9*). Curves C (Fig. 5) represent in all cases a steady value of the activity. The activity decreases in the order:

$$\text{NiO(250)} \geq \text{NiO(Ga)(250)} > \text{NiO(Li)(250)} > \text{NiO(200)}$$

The differences in activity are not correlated exclusively with different poisoning effects by adsorbed carbon dioxide since the same sequence of activities is evident also from curves A (Fig. 5), which were obtained during the first introductions of reaction mixture, i.e., when the surface is not yet inhibited by carbon dioxide. A test carried out in a static reactor confirms the sequence of activities (Fig. 6). NiO(250) and NiO(Ga) (250), on which Mechanism II prevails, are the most active catalysts, whereas Mechanism I, the only mechanism which is probable on NiO(Li) (250) and NiO(200), appears to be responsible for a decreased catalytic activity.

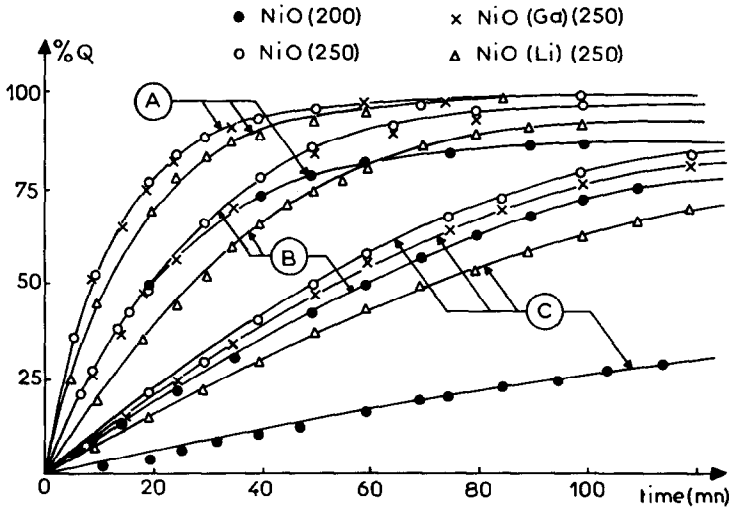

FIG. 5. Rates of production of heat during the reaction of doses of the stoichiometric mixture ($CO + \frac{1}{2} O_2$) on the different nickel oxide samples at 30°C. Dose A of mixture after conversion of 3 cm^3 of reaction mixture per gram of catalyst; dose B after conversion of 7 cm^3; dose C after conversion of 20 cm^3 (steady state).

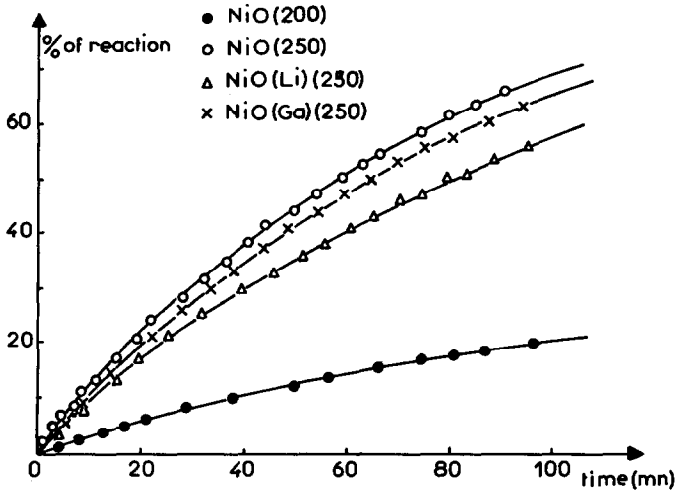

FIG. 6. Kinetic curves for the oxidation of carbon monoxide at 30°C on four catalysts in a static reactor.

CONCLUSIONS

It is of interest to compare these results with those obtained by Dell and Stone (*17*) in a study of the chemisorption and of the interactions of gases, at 20°C, on the surface of nickel oxide samples prepared by the partial oxidation of finely divided nickel metal at 300°C. Oxygen is chemisorbed in a very similar way on the metal-supported nickel oxide and on the samples prepared in this work from the hydroxide, although chemisorption of carbon monoxide and carbon dioxide occurs to a larger extent on our samples than on the metal-supported oxide. Interaction of oxygen with preadsorbed carbon monoxide yields, in both cases, a CO_3 complex (Eq. [2]). Reactivity towards carbon monoxide of the CO_3 complex formed on the metal-supported nickel oxide is either nil or very small. On our samples, however, reactivity of the similar complex is observed, but, from the analysis of the calorimetric data, it has been shown that the reactivity of this complex depends on its energy of formation. Indeed, a fraction of these complex ions formed, for instance, on NiO(200) is not active towards carbon monoxide (*13*), and, as in the case of the metal-supported samples, this fraction inhibits the oxide surface. It has been postulated that on NiO(200) the most active surface sites, on which nonreactive CO_3^- ions are most probably adsorbed, are exposed nickel ions (*15*). It is likely, therefore, that on the metal-supported nickel oxides prepared by Dell and Stone active surface nickel ions are in a protruding position. The interaction between preadsorbed oxygen and carbon monoxide, which on the metal-supported nickel oxide again yields exclusively the CO_3 complex, produces on our samples either a similar complex or carbon dioxide (gaseous or adsorbed) (Eqs. [6] and [7]), depending on the energy of the adsorption of oxygen (Tables 7, 8, and 9). Since the formation of the complex ions during interaction [6] has been related, in our case, to the chemisorption of oxygen on anionic vacancies [case of NiO(250) and NiO(Li) (250)] (*6*), it may be deduced that anionic vacancies also exist on the surface of the metal-supported nickel oxides studied by Dell and Stone (*17*). Moreover, it is reasonable to assume that exposed nickel ions and anionic vacancies may coexist on a nickel oxide surface. It may be inferred, therefore, that the surface of the catalyst used in the study of ref. (*17*) was not only stripped of excess oxygen either by desorption or, more probably, by incorporation, during the outgassing treatment at 380°C *in vacuo* which was carried out before the chemisorption experiments, but that it actually became oxygen-deficient. If this was

the case, one should expect the remaining surface lattice oxygen ions to be strongly coordinated. This would then explain, as suggested by Stone (*18*), the differences between the chemisorption of carbon monoxide and carbon dioxide on the samples prepared either by oxidation of the metal or by dehydration of the hydroxide, since strongly coordinated surface oxygen ions would present a small affinity towards carbon monoxide or carbon dioxide; whereas interactions between these gases and surface oxygen ions do occur on our samples, as shown by isotopic exchange experiments conducted at room temperature (*19, 20*). Surface oxygen anions on our samples are, however, still too strongly coordinated to oxidize carbon monoxide to carbon dioxide at room temperature and they do not take part in the catalytic combustion of carbon monoxide at 30°C (*20*).

Finally, it must be noted that the catalytic activity of nickel oxides prepared by the low-temperature dehydration *in vacuo* of the hydroxide is not related to their initial electrical conductivity since, in particular, NiO(200) and NiO(250), which present the largest difference in activity, have the same electrical properties. It is not related either to the total stoichiometry of the samples since the stoichiometries of NiO(Li)(250) and NiO(Ga)(250) are very different (Table 1) but their catalytic activities are similar. Changes of activity may be correlated, from our calorimetric data, with the occurrence of two reaction mechanisms (I and II). This rules out any simple correlation between the catalytic activity and the electronic structure of the four catalysts. Mechanism I, which includes the intermediate formation of CO_3^-(ads) ions, is possible on all four catalysts but operates actually on NiO(200) and NiO(Li)(250). The probability of Mechanism II, which is faster than Mechanism I, may be related to the energy of the bond between adsorbed oxygen and surface nickel ions.

As is evident from Fig. 1, the energy distribution of the bonds between adsorbed oxygen and surface nickel ions varies with the mode of preparation of the catalysts and with their composition. The decrease of the bond energy which is observed on a fraction of the NiO(250) surface compared with the NiO(200) surface probably results from the recession of nickel ions due to a higher temperature of preparation (*15*). This decrease is responsible for the change of reaction mechanism from Mechanism I to Mechanism II, since less strongly bound oxygen ions on NiO(250) present a greater reactivity towards carbon monoxide and since gaseous carbon dioxide is directly produced by this interaction (Mechanism II). On the contrary, the same interaction on the unrecessed nickel ions of the NiO(200) surface produces adsorbed carbon dioxide exclusively, which inhibits the catalyst, and the reaction mechanism necessitates the intermediate formation of a CO_3^-(ads) complex (Mechanism I).

As a result of the incorporation *in vacuo* of lithium ions, it has already been shown that the bond energy between adsorbed oxygen and the surface of the nickel oxide increases (Fig. 1) (*3, 6*). The surface properties of the lithiated nickel oxide have been explained by an increased number of anionic vacancies. When oxygen is adsorbed on these high-energy sites, it has a small reactivity and, therefore, Mechanism I controls again the catalytic reaction on NiO(Li)(250).

Incorporation of gallium ions into the surface lattice layers of nickel oxide *in vacuo* at 250°C decreases the affinity of the solid towards oxygen because cationic vacancies are formed which are inactive towards this gas and because recession of surface cations decreases the energy of adsorption of oxygen (*6*). On NiO(Ga)(250), as on NiO(250), Mechanism II therefore presents a lower energy barrier than Mechanism I and a greater probability.

Finally, it appears that when oxygen is adsorbed on anionic vacancies (high-energy sites) (*6*), interaction with carbon monoxide yields the intermediate CO_3^-(ads) ions. On medium-energy sites, the same interaction produces adsorbed carbon dioxide. On low-energy sites, which are probably par-

tially recessed nickel ions (*15*), desorption of carbon dioxide occurs. It therefore seems that the catalytic activity of highly divided nickel oxides is better explained by local surface properties than by collective or average properties.

REFERENCES

1. STONE, F. S., *Advan. Catalysis* **13**, 1 (1962).
2. MERLIN, A., AND TEICHNER, S. J., *Compt. Rend.* **236**, 1892 (1953).
3. EL SHOBAKY, G., GRAVELLE, P. C., AND TEICHNER, S. J., *Bull. Soc. Chim. France,* pp. 3244, 3251 (1967).
4. EL SHOBAKY, G., GRAVELLE, P. C., TEICHNER, S. J., TRAMBOUZE, Y., AND TURLIER, P., *J. Chim. Phys.* **64**, 310 (1967).
5. GRAVELLE, P. C., EL SHOBAKY, G., AND URBAIN, H., *Compt. Rend.* **262**, 549 (1966).
6. EL SHOBAKY, G., GRAVELLE, P. C., AND TEICHNER, S. J., Symposium on Electronic Phenomena in Chemisorption and Catalysis on Semiconductors, Moscow, 1968, to be published.
7. GRAVELLE, P. C., *J. Chim. Phys.* **61**, 455 (1964).
8. ARGHIROPOULOS, B., AND TEICHNER, S. J., *J. Catalysis* **3**, 477 (1964).
9. TEICHNER, S. J., MARCELLINI, R. P., AND RUE, P., *Advan. Catalysis* **9**, 458 (1957); MARCELLINI, R. P., RANC, R. E., AND TEICHNER, S. J., *Actes Congr. Intern. Catalyse, 2e, Paris, 1960,* p. 289 (Technip, Paris, 1961); COUE, J., GRAVELLE, P. C., RANC, R. E., RUE, P., AND TEICHNER, S. J., *Proc. Intern. Congr. Catalysis, 3rd, Amsterdam, 1964,* p. 748 (North-Holland Publ. Co., Amsterdam, 1965).
10. CHARMAN, H. B., DELL, R. M., AND TEALE, S. S., *Trans. Faraday Soc.* **59**, 469 (1963).
11. EL SHOBAKY, G., GRAVELLE, P. C., AND TEICHNER, S. J., *Colloq. Intern. Centre Natl. Rech. Sci. (Paris)* **156**, 175 (1967).
12. EL SHOBAKY, G., GRAVELLE, P. C., AND TEICHNER, S. J., *Bull. Soc. Chim. France,* to be published.
13. GRAVELLE, P. C., AND TEICHNER, S. J., *J. Chim. Phys.* **61**, 527, 533, 625 (1964).
14. "Selected Values of Chemical Thermodynamic Properties." *Natl. Bur. Std. Circ.* **500** (1952).
15. EL SHOBAKY, G., GRAVELLE, P. C., AND TEICHNER, S. J., Oxidation of Organic Compounds. *Advan. Chem. Series* **76**, 292 (1968).
16. COUE, J., Thesis, n° 149, Lyon, 1963.
17. DELL, R. M., AND STONE, F. S., *Trans. Faraday Soc.* **50**, 501 (1954).
18. STONE, F. S., *Actes Congr. Intern. Catalyse, 2e, Paris, 1960,* p. 323 (Technip, Paris, 1961).
19. KLIER, K., AND HERMAN, Z., *Coll. Czech. Chem. Commun.* **29**, 2556 (1964); KLIER, K., AND JIRATOVA, M., *Proc. Intern. Congr. Catalysis, 3rd, Amsterdam, 1964,* p. 763 (North-Holland Publ. Co., Amsterdam, 1965).
20. BAILLY, J. C., GRAVELLE, P. C., AND TEICHNER, S. J., *Bull. Soc. Chim. France,* p. 1620, (1967); BAILLY, J. C., AND TEICHNER, S. J., *Bull. Soc. Chim. France,* p. 2376 (1967).